Citation: (Submitted version) Fenaux, M.; Reyes, E.; Galvez, J. C.; Moragues, A.;2019.
Modelling the transport of chloride and other ions in cement-based materials. Cement & Concrete
Composites. 97 33-42, 2019, ISSN: 0958-9465, DOI: 10.1016/j.cemconcomp.2018.12.009

Modelling the transport of chloride and other ions in cement-based materials

M. Fenaux[a], E. Reyes[a], J.C. Gálvez[a,*], A. Moragues[a]

[a] *Universidad Politécnica de Madrid*
Escuela de Ingenieros de Caminos, Canales y Puertos (Civil Engineering School)
Madrid 28040, Spain

Abstract

Research on mechanisms of chloride ion transport in cement based materials is relevant to improve the durability of reinforced concrete structures. Traditional chloride transport models consider a linear diffusion equation, only valid for fully saturated and non-reactive concrete. This work proposes a model of chloride and other ions penetration in saturated concrete considering diffusion, chloride binding, chemical activity and migration. The model uses intrinsic diffusion coefficients. The influence of the ionic pore solution on chloride penetration in concrete is also studied. The chemical activity is introduced by coupling the transport equations to the Pitzer model. The migration is accounted for by imposing the electro-neutrality condition of the pore solution. It is shown that fitting the well known error function to experimentally obtained chloride profiles present results which are difficult to interpret. Moreover, it is shown that, accounting for solely diffusion and chloride binding, good results are obtained. Contemplating chemical activity and migration slightly improves those results and allows the determination of the concentration profiles of the present ionic species in the pore solution, which are involved in the degradation processes of cement-based materials exposed to aggressive environments.

Keywords: Chloride transport, Modelling, Diffusion coefficients, Pitzer model, Ionic pore solution

1. Introduction

Reinforced concrete is one of the most widely used structural materials as it combines the good structural properties, ease of manufacturing and relatively low cost of concrete, with the use of embedded steel reinforcing bars to overcome the weakness in tension. Apart from sufficiently high mechanical strength this material must be adequately resistant to the potential aggressiveness of the environment during its service life. Therefore, the durability of reinforced concrete is one of the most important areas of research interest. Concrete and other cementitious materials are quite reactive media that may be significantly altered from the contact with an aggressive environment. These materials are composed of aggregates of different sizes held together by a porous binder, a mix of solids and pores called hydrated cement paste (1). So, pores are inherent to concrete, which can also be produced as a result of an inadequate compaction. This pore system governs the most important properties of concrete, notably its strength and durability, as the ingress of any aggressive substance is determined by its porous structure, especially the accessible part. Porosity and interconnectivity are controlled for the most part by the w/c ratio, the degree of hydration, and the degree of compaction (2). The permeability of concrete is a challenging field of study, since concrete is a heterogeneous blend of materials which properties change with age. In these materials three main phases in equilibrium can be distinguished: aqueous, solid, and gaseous. The aqueous phase, occupying a portion of the porous network, is a highly charged ionic solution containing mainly the following species in different concentrations depending on the cementitious material (3): OH^-, Na^+, K^+, SO_4^{2-} and Ca^{2+}. The solid phase is a composite mixture of hydrated calcium silicates gels (C-S-H) and other crystalline phases like portlandite ($Ca(OH)_2$). When the pore solution is disturbed, frequently due to aggressives coming from the external environment, an amount of one or more solid phases might be either dissolved or precipitated in order to reach back the equilibrium state and consequently the durability of concrete might be affected. The gaseous phase is a mixture of dry air and water vapor, which does not contain ions. The pressure difference between the gaseous and the aqueous phase caused by a drying of the material provokes capillary suction. As a consequence, a movement of water takes place, resulting in an advection effect on the ions of the pore solution. Therefore, the accessible porosity and its connectivity are critical with respect to the movement of water and chemical substances into and out of the reinforced concrete, as porosity is connected to many deterioration processes driven by the transport properties of concrete, involving both the concrete and the steel.

It is generally accepted that chloride penetration into concrete is one of the main causes of steel corrosion and premature failure for reinforced concrete structures during service life. Chloride induced corrosion of reinforced and prestressed concrete typically occurs in marine environments, or when the concrete is exposed to deicing salts. This involves

*Corresponding author
Email address: jaime.galvez@upm.es (J.C. Gálvez)

high maintenance and repairing costs (4, 5, 6). Consequently, studying the processes involved in chloride induced corrosion is of utmost benefit. For that reason, published research on durability of concrete against chlorides has enjoyed substantial interest in recent years (7, 8, 9).

Accurate prediction of the behaviour of concrete in environments with chlorides has been a challenge until now. An enormous variety of mathematical models has been proposed over the years with the main goal to explain and predict the penetration of chloride ions into concrete. Most of the models are simplistic and reduce to a simple apparent diffusion equation. On this approach are based the most common diffusion standardized tests (1, 3), among others. Some proposed models are more consistent with the physics of the phenomena by considering chloride absorption (10, 11, 12, 13, 14), but some incongruous approximations still remain. For example, the models reported in the literature which consider the dependence on the pore solution composition are still few (15, 16). Chloride diffusion is particularly dependent on hydroxyls and cations. Recently, Yang and Wang (17) have proposed a formula by up-scaling to correlate the effective chloride ion diffusivity with electrokinetic effect in cement paste.

The frequently used apparent diffusion coefficient accounts for several physical phenomena, such as chloride binding. However, studying each phenomenon individually allows the use of intrinsic material parameters, which is shown in this work. The most basic chloride transport models consider a linear diffusion equation (18, 19):

$$\frac{\partial C}{\partial t} = D_e \nabla . (\nabla C) \tag{1}$$

where C is the free chloride concentration (kg/m^3 of pore solution) and D_e the so called effective or intrinsic diffusion coefficient (m^2/s), a concept introduced in (20). Equation 1 is valid for fully saturated and non-reactive concrete. Furthermore, the interactions between several ionic species are ignored. In order to describe the diffusion of the free and total chloride ions, that is, taking into account the bound chloride content, Saetta et al. (10) used two kinds of diffusion coefficients, namely the effective or intrinsic diffusion coefficient D_e and the apparent diffusion coefficient D_a, both expressed in m^2/s. Denoting the total and free chloride concentrations as C_t and C_f, both expressed in kg/m^3 of concrete, the diffusion equations are given by:

$$\frac{\partial C_t}{\partial t} = \nabla . \left(D_e \nabla C_f \right) \tag{2}$$

$$\frac{\partial C_t}{\partial t} = \nabla . (D_a \nabla C_t) \tag{3}$$

Denoting the bound chloride concentration as C_b, such that $C_t = C_f + C_b$, and assuming that C_b is a function of the free chloride concentration C_f , the effective and apparent diffusion coefficients are related by the following equation:

$$D_a = \frac{D_e}{1 + \frac{dC_b}{dC_f}} \tag{4}$$

Chloride binding depends on many factors, such as temperature (13), the alkalinity of the pore solution (20) and carbonation (21). Part of the chloride anions present in cementicious materials can be bound to the cement in two ways, namely by a chemical bond with the hydration products (22, 14, 12, 11, 23) or by a physical adsorption onto the calcium silicate hydrate phases (14, 24, 25, 26).

Coussy and Ulm (27) proposed a diffusion-reaction model contemplating the chloride binding:

$$\frac{\partial (\phi C)}{\partial t} + \frac{\partial ([1 - \phi] C_b)}{\partial t} = \nabla . (\phi D_e \nabla C) \tag{5}$$

where ϕ is the porosity and $(1 - \phi)$ corresponds to the relative volume of solid material. A value of $2.3 \times 10^{-12} m^2/s$ was adopted for ϕD_e. Equation 5 is valid for saturated concrete ($\phi_l = \phi$). Samson et al. (28) derived the mass transport equations using the homogenization technique. They described the transport and mass conservation equations at the microscopic scale, which were then averaged over the entire volume of the bulk material. Consequently, the following chloride ion transport model for fully saturated and non-reactive concrete was proposed:

$$\frac{\partial C}{\partial t} = \nabla . \left(D_e \nabla C - \frac{F D_e}{RT} C \nabla \Phi \right) \tag{6}$$

where R, F and T are the gas and the Faraday constants and the temperature, respectively, and Φ the electric potential which can be calculated by means of the Poisson equation for electrostatics. Equation 6 is known as the Nernst-Planck equation at the macroscopic scale. The second term on the right-hand side of Equation 6 is due to the fact that the diffusion of chloride ions in porous materials is of an ionic and not molecular nature, and takes the migration mechanism into account.

The extended Nernst-Planck equation is obtained by summing a term to equation 6 which accounts for the chemical activity:

$$\frac{\partial C}{\partial t} = \nabla . \left(D_e \nabla C + D_e \frac{C}{\gamma} \nabla \gamma - \frac{F D_e}{RT} C \nabla \Phi \right) \tag{7}$$

where γ is the activity coefficient.

The activity coefficient was examined in (29). The authors proposed a modified expression for the effective diffusion coefficient in order to account for the chemical activity based on the extended Debye-Hückel model. However, it is shown in (28) that the extended Debye-Hückel is valid only for low concentrations (up to $100 mmol/l$). According to the research works presented in (28, 30), the most suitable model for the calculation of the activity coefficient is the Pitzer model (31). The Debye-Hückel, extended Debye-Hückel or the Davies

models are often preferred due to their simplified formulation (32).

The electrical potential can be calculated by means of Poisson's equation for electrostatics (28, 16) or by imposing the electroneutrality condition on the pore solution, the latter being a technique used in (33).

The mass fluxes of an ionic species i in the pore solution can be obtained by computing the gradient of the electrochemical potential (34):

$$\boldsymbol{J}_D = -D_i \nabla C_i \quad \text{(diffusive flux)} \tag{8}$$

$$\boldsymbol{J}_a = -D_i \frac{C_i}{\gamma_i} \nabla \gamma_i \quad \text{(advective flux)} \tag{9}$$

$$\boldsymbol{J}_T = -\frac{D_i}{T} C_i \ln a_i \nabla T \quad \text{(temperature flux)} \tag{10}$$

$$\boldsymbol{J}_\Phi = -D_i \frac{z_i F}{RT} C_i \nabla \Phi \quad \text{(electric flux)} \tag{11}$$

where D_i refers to the effective diffusion coefficient of species i, C_i the concentration of species i, γ_i the activity coefficient, T the temperature and a_i the dimensionless chemical activity of species i.

Many models for predicting chloride penetration in concrete are based on these mass fluxes. For instance, the linear diffusion equation 1 can be derived by ignoring the mass fluxes $\boldsymbol{J}_a$, $\boldsymbol{J}_T$ and $\boldsymbol{J}_\Phi$, assuming that diffusion is the predominant transport mechanism.

Substituting these mass fluxes into the continuity equation, the following transport model is obtained:

$$\frac{\partial C_i}{\partial t} = \nabla . \left(D_i \nabla C_i + D_i \frac{C_i}{\gamma_i} \nabla \gamma_i + \frac{D_i}{T} \ln a_i C_i \nabla T + D_i \frac{z_i F}{RT} C_i \nabla \Phi \right) + f_i \tag{12}$$

where f_i acts as a source if $f_i > 0$ and as a sink if $f_i < 0$.

This work proposes a multiionic transport model for saturated materials dedicated specifically to chloride transport cementitious materials, but that eventually may be used to predict the behaviour of concrete in several environments. The chloride transport model presented in this work considers the mass fluxes caused by the electric and temperature fluxes, apart from the diffusive flux and differs from other models in that it is coupled to the Pitzer model in order to account for the chemical activity, dependent on pore solution composition. Furthermore, it is coupled to the transport equations for all the main chemical species present in the pore solution.

In practice, it is very common to predict chloride penetration with a simple diffusion equation, using a constant apparent diffusion coefficient. The solution of this equation is usually fitted to experimental data in order to calculate the apparent diffusion coefficient. In this work, it is shown that such a model may lead to non-accurate results in some cases and that the value of the apparent diffusion coefficient is difficult to interpret. Several models for chloride penetration into hardened concrete are revised and compared with experimental data. For the sake of simplicity, the analysis is carried out for fully saturated concrete under isothermal conditions. In other words, advective mass fluxes as well as $\boldsymbol{J}_T$ are not considered here.

The chloride transport model presented in this work differs from other models in that it is coupled to the Pitzer model in order to account for the chemical activity. Furthermore, it is coupled to the transport equations for all the main chemical species present in the pore solution.

Instead of modifying the diffusion coefficient for considering the effects of chemical reactions, physical absorption or chemical activity, the authors propose to model each mass flux independently which allows the use of intrinsic diffusion coefficients which do not depend on the concentration of the ionic species.

2. General considerations

Throughout this work, the free concentration of species i expressed in kg/m^3 or g/l of pore solution and in kg/m^3 of concrete are denoted as C_i and C_{fi}, respectively. The bound concentration of species i expressed in kg/m^3 of concrete is denoted as C_{bi}. The total chloride concentration C_{ti} of species i can then be written as:

$$C_{ti} = C_{fi} + C_{bi} = \phi C_i + C_{bi} \tag{13}$$

where ϕ is the porosity expressed in m^3/m^3 of concrete. When the subscript i is omitted, C_t, C_f, C and C_b refer to the concentrations of chloride ions. All the diffusion coefficients are expressed in m^2/s.

As mentioned before, the present analysis is carried out under isothermal conditions. Furthermore, the material is assumed to be infinitely rigid and homogeneous. However, the porosity ϕ can change under influence of chloride binding as will be discussed in more detail below.

3. Materials and methods

In this work, two concretes are studied. The cement type used for both materials was Portland cement *EN 197-1-CEM I 42.5-SR5* (35). This cement was used in the design of two different concrete mixes: one without admixtures and one by using cement Type I plus silica fume, as cement replacement. In this latter case a replacement of ten per cent relative to the weight of cement was used, within the limits allowed by the current Spanish standards. The authors followed the recommendations of the EHE (36), replacing the cement contents (C) with cementitious material ($C + KF$),

where F was the content of the admixture and K the coefficient of effectiveness. In this work $K = 2$ is used for the silica fume. The concrete mixtures were prepared with a water-to-cementitious materials ratio (w/cm) of 0.45. The fine aggregate used was a natural siliceous sand with a 2.8 fineness modulus. The coarse aggregate was crushed limestone with a maximum size of 20 mm and a 6.88 fineness modulus. With the aim of achieving an appropriate workability, a superplasticizer was used as a high-range water-reducing agent.

From now on, the concrete without admixtures is referred to as material SR (sulfate-resisting), while the other one is referred to as material SF (silica fume). The materials were elaborated and thoroughly tested in the research work (37). Table 1 shows the compositions of the mixtures.

Table 1: Dosage of materials SR and SF in kg/m^3.

Material	SR	SF
Cement	380	304
Silica fume	0	38
Water	171	154
Water/binder ratio	0.45	0.45
Sand	787	800
Coarse Aggregate	1022	1067
Superplasticizer	0.97	1.80

The porosity of each material was obtained by measuring the difference in weight beween oven dried and water saturated concrete samples. The dry and water saturated samples were obtained respectively by drying them at $50°C$ and sumberging them in tap water at $20°C$ until no change in mass greater than 0.1% of the initial mass was recorded within a time interval of minimum 24 hours. In order to determine the chloride transport properties of the materials, the latter were subjected to a 3% *NaCl* solution 28 days after casting, as instructed by the standard *ASTM C1543-02* (38). In a previous research work (37), the total chloride concentration C_t was measured according to the standard test method *UNE-112010:1994* (39) at several depths and after 182, 364 and 546 days of chloride penetration. For a more detailed explanation of the procedure, the reader is referred to (37).

In the research work (34), the free chloride concentration C_f of the same concrete samples was measured experimentally following the indications of the proceeding *Recommendations of RILEM TC 178-TMC* (40). Subtracting the free chloride concentration from the total concentration, the bound concentrations was determined. The Langmuir model was used to establish a mathematical relation between the bound and the free concentrations:

$$C_b = C_{bm}\frac{K_{eq}C_f}{1 + K_{eq}C_f} \tag{14}$$

where C_{bm} is the maximum concentration of bound chlorides (kg/m^3 of concrete), and K_{eq} is the equilibrium constant of the following reaction equation:

$$free\ Cl^- + free\ sites \leftrightharpoons bound\ Cl^- \tag{15}$$

$$C_f + (C_{bm} - C_b) \leftrightharpoons C_b \tag{16}$$

Fitting equation 14 to the experimental data, the values of C_{bm} and K_{eq} were obtained for both materials. For a more detailed description of the determination of the free and bound chloride concentration, the reader is referred to (34).

4. Modelling of chloride transport in saturated concrete

4.1. Apparent diffusion

The apparent diffusion model of chloride ions in concrete is based on the diffusive flux (equation 8). Substitution of the latter into the continuity equation yields:

$$\frac{\partial C_t}{\partial t} = \nabla.(\phi D_e \nabla C) \tag{17}$$

It is of common use to express the bound chloride concentration as a function of the free chloride concentration (see for instance (41)). In that case, equation 17 can be rewritten in terms of the apparent diffusion coefficient D_a:

$$\frac{\partial C_t}{\partial t} = \nabla.(D_a \nabla C_t) \tag{18}$$

Comparing equations 17-18, and assuming that ϕ is constant, the relation between the effective and apparent diffusion coefficients is obtained.

$$D_a = \frac{D_e}{1 + \frac{dC_b}{dC_f}}, \qquad \text{if } C_b = C_b(C_f) \tag{19}$$

$$D_a = \frac{D_e}{1 + \frac{1}{\phi}\frac{dC_b}{dC}}, \qquad \text{if } C_b = C_b(C) \tag{20}$$

Equation 17 can be written as a function of C_f instead of C_t:

$$\frac{\partial C_f}{\partial t} = \frac{1}{1 + \frac{dC_b}{dC_f}}\nabla.\left(D_e \nabla C_f\right) \tag{21}$$

If D_e is constant, equations 21 becomes:

$$\frac{\partial C_f}{\partial t} = D_a \nabla.\left(\nabla C_f\right) \tag{22}$$

where D_a is defined by equations 19-20.

It is worthwhile to note that D_a is not an intrinsic diffusion coefficient as it strongly depends on the chloride binding and therefore on the chloride concentration itself. For non-linear chloride binding, assuming that D_a is constant leads to erroneous results. Indeed, it is shown below that fitting equation 17 to experimental data at several times leads to very different values of D_a. Furthermore, given an apparent diffusion coefficient, it is difficult to determine whether the value is due to the microstructure or to the binding capacity of the concrete. Based on these reasons and from practical point of view it is recommended to obtain D_a under similar conditions to those that will be applied. Moreover, it is quite difficult to directly compare the values of D_a obtained from different standards.

4.2. Effective diffusion

The effective diffusion model is based on the diffusive flux (equation 8) as well. The main difference with the apparent diffusion model is that it accounts for diffusion and chloride binding separately:

$$\frac{\partial C_f}{\partial t} = \nabla.(\phi D_e \nabla C) + f \tag{23}$$

where f is the source/sink term which accounts for chloride binding.

Subtracting equation 23 from equation 17 and using the relation 13, the following expression for f is obtained:

$$f = -\frac{dC_b}{dC_f}\frac{\partial C_f}{\partial t} \tag{24}$$

where C_b is assumed to depend solely on C_f. Substitution of equation 24 into equation 23 yields:

$$\left(1 + \frac{dC_b}{dC_f}\right)\frac{\partial C_f}{\partial t} = \nabla.(\phi D_e \nabla C) \tag{25}$$

Note that equation 25 is equivalent to equation 18 if the apparent diffusion coefficient is defined by equation 19. If diffusion and chloride binding are the only transport mechanisms, then D_e is an intrinsic diffusion coefficient of chloride ions in homogeneous concrete (in isothermal conditions).

4.3. Diffusion, activity and migration

The diffusion-activity-migration model involves substituting the mass fluxes (equations 8, 9 and 11) into the continuity equation:

$$\left(1 + \frac{dC_b}{dC_f}\right)\frac{\partial C_f}{\partial t} = \nabla.\left(D_e \nabla C_f + D_e \frac{C_f}{\gamma}\nabla\gamma - \frac{F D_e}{RT} C_f \nabla\Phi\right) \tag{26}$$

As the activity coefficient and electric potential depend on all the ionic species present in the pore solution, the evolution with time of all those species need to be calculated. Therefore, a transport equation for each species is needed:

$$\left(1 + \frac{dC_{bi}}{dC_{fi}}\right)\frac{\partial(\phi C_i)}{\partial t} = \nabla.\left(\phi D_i \nabla C_i + \phi D_i \frac{C_i}{\gamma_i}\nabla\gamma_i + \phi D_i \frac{z_i F}{RT} C_i \nabla\Phi\right) \tag{27}$$

The activity coefficient depends on the ionic strength and the interactions between all the ionic species (42, 43). One of the most known models to calculate the activity of an ionic species in a given solution is based on the Debye-Hückel theory (44). This theory has been improbed resulting in more accurate models such as the extended Debye-Hückel model and the Davies equation (32). However, these models are only valid for low concentrations. An alternative is the Pitzer model which is valid for high concentrations and accounts not only for the ionic strenght of the solution, but also for the interaction between the ions by means of interaction parameters. According to the Pitzer model, the activity coefficients of a cation X and an anion Y can be calculated as follows:

$$\begin{aligned}\ln\gamma_X = {} & z_X^2 F_\gamma + \sum_{an} m_{an}\left(2B_{X,an} + ZC_{X,an}\right) \\ & + \sum_{cat} m_{cat}\left(2\Theta_{X,cat} + \sum_{an} m_{an}\Psi_{X,cat,an}\right) \\ & + \sum_{an}\sum_{an'\neq an} m_{an}m_{an'}\Psi_{an,an',X} \\ & + |z_X| \sum_{cat}\sum_{an} m_{cat}m_{an}C_{cat,an}\end{aligned} \tag{28}$$

$$\begin{aligned}\ln\gamma_Y = {} & z_Y^2 F_\gamma + \sum_{cat} m_{cat}\left(2B_{cat,Y} + ZC_{cat,Y}\right) \\ & + \sum_{an} m_{an}\left(2\Theta_{X,an} + \sum_{cat} m_{cat}\Psi_{Y,an,cat}\right) \\ & + \sum_{cat}\sum_{cat'\neq cat} m_{cat}m_{cat'}\Psi_{cat,cat',Y} \\ & + |z_Y| \sum_{cat}\sum_{an} m_{cat}m_{an}C_{cat,an}\end{aligned} \tag{29}$$

where the subscripts *cat* and *an* refer to cation and anion. The concentration of each ionic species is denoted by m in molal units. F_γ depends on the ionic strength $I = \frac{1}{2}\sum_i m_i z_i^2$. The matrixes B, C, Θ and Ψ contain the interaction parameters between the ions present in the solution and $Z = \sum_i m_i z_i^2$ is the modified ionic strength. A detailed description of the Pitzer model can be found in (31, 45, 46, 47). Note that the Pitzer model requires the concentration of the species in molal units, while the transport model expressed the concentration in g/l. To convert molal units to g/l and vice versa, the density of the pore solution, which depends on the concentrations of the ionic species, needs to be calculated. In this work, it is assumed that the density depends solely on the *NaCl* concentration as follows (48):

$$\rho = 1000 + \rho_{20}\varepsilon C_{NaCl} \tag{30}$$

where ρ is the density of the pore solution (g/l), $\rho_{20} = 998.2 g/l$ is the density of water at $20°C$, $\varepsilon = 6.46 \times 10^{-4} l/g$ is a correlation coefficient and C_{NaCl} is the concentration of dissolved $NaCl$ (g/l).

Since the activity coefficients can be expressed as a funtion of the concentrations of the ionic species, the flux 9 can be rewritten as:

$$\boldsymbol{J}_a = -D_i\frac{C_i}{\gamma_i}\nabla\gamma_i = -D_i\frac{C_i}{\gamma_i}\sum_j \frac{\partial\gamma_i}{\partial C_j}\nabla C_j \tag{31}$$

The electric field $\boldsymbol{E} = -\nabla\Phi$ acts in such a way that the sum of all the electric charges equals zero everywhere and at any time. The electric field can be calculated by solving the Poisson equation for electrostatics. However, it can be calculated without adding a variable to the model, namely by imposing the electroneutrality of the pore solution. The current density I

(A/m^2) in the pore solution is obtained directly from the mass fluxes 8, 9 and 11:

$$I = \sum_i \frac{z_i F}{M_i}\left(\boldsymbol{J}_D^i + \boldsymbol{J}_a^i + \boldsymbol{J}_\Phi^i\right) \tag{32}$$

where M_i is the molar mass of species i. Setting I to zero, the electric field is obtained:

$$\boldsymbol{E} = -\nabla\Phi = \frac{RT}{F}\frac{\sum_i \frac{z_i}{M_i}\left(D_i\nabla C_i + D_i\frac{C_i}{\gamma_i}\sum_j \frac{\partial\gamma_i}{\partial C_j}\nabla C_j\right)}{\sum_i \frac{z_i^2}{M_i}D_i C_i} \tag{33}$$

5. Solution of the differential equations

The analytic solution of the apparent diffusion model is:

$$C_t(t,x) = C_{t0} + (C_{ts} - C_{t0})\,erfc\left(\frac{x}{\sqrt{4D_a t}}\right) \tag{34}$$

where $C_{t0} = C(0,x)$ and $C_{ts} = C(t,0)$. Note that equation 34 is a solution of equation 18 if and only if C_{ts}, C_{t0} and D_a are constant. Furthermore, equation 34 is obtained by integration equation 18 on a semi-infinite domain ($x \in [0,\infty[$). The assumption of a constant D_a is only valid if the bound chloride concentration is at most a linear function of the free chloride concentration.

The effective diffusion model and the diffusion-activity-migration model were solved by means of the standard finite element method (Galerkin formulation). The time derivatives were discretized by means of the implicit Euler method. Only the matrix formulation of the third problem is presented here.

Consider n ionic species dissolved in the pore solution. The natural boundary conditions are taken to be:

$$(\nabla C_i)^T \cdot \boldsymbol{n} = 0 \quad \forall i = 1,\ldots,n \quad \text{on } \boldsymbol{\Gamma}_N \tag{35}$$

where $\boldsymbol{\Gamma}_N$ is the Neumann boundary and $\boldsymbol{n}$ is the normal vector to $\boldsymbol{\Gamma}_N$. Applying the natural boundary conditions to the weak formulation, the matrix equations of the problem are obtained:

$$\begin{bmatrix} \boldsymbol{M}_{11} & \boldsymbol{M}_{12} & \ldots & \boldsymbol{M}_{1n} \\ \boldsymbol{M}_{21} & \boldsymbol{M}_{22} & \ldots & \boldsymbol{M}_{2n} \\ \vdots & \ddots & & \vdots \\ \vdots & & \ddots & \vdots \\ \boldsymbol{M}_{n1} & \boldsymbol{M}_{n2} & \ldots & \boldsymbol{M}_{nn} \end{bmatrix}\begin{bmatrix} \dot{\boldsymbol{C}}_1 \\ \dot{\boldsymbol{C}}_2 \\ \vdots \\ \vdots \\ \dot{\boldsymbol{C}}_n \end{bmatrix} + \begin{bmatrix} \boldsymbol{K}_{11} & \boldsymbol{K}_{12} & \ldots & \boldsymbol{K}_{1n} \\ \boldsymbol{K}_{21} & \boldsymbol{K}_{22} & \ldots & \boldsymbol{K}_{2n} \\ \vdots & \ddots & & \vdots \\ \vdots & & \ddots & \vdots \\ \boldsymbol{K}_{n1} & \boldsymbol{K}_{n2} & \ldots & \boldsymbol{K}_{nn} \end{bmatrix}\begin{bmatrix} \boldsymbol{C}_1 \\ \boldsymbol{C}_2 \\ \vdots \\ \vdots \\ \boldsymbol{C}_n \end{bmatrix} = \begin{bmatrix} \boldsymbol{0} \\ \boldsymbol{0} \\ \vdots \\ \vdots \\ \boldsymbol{0} \end{bmatrix} \tag{36}$$

where each matrix $\boldsymbol{M}_{ij}$ and $\boldsymbol{K}_{ij}$ have dimensions $nod \times nod$ where nod denotes the number of nodes of the mesh. The vectors $\boldsymbol{C}_i = [C_i^{(1)} C_i^{(2)} \ldots C_i^{(nod)}]^T$ contain the nodal values.

Let the vector of shape functions be $\boldsymbol{N} = [N_1, N_2, \ldots, N_n]$ and Ω the spatial domain, then, for the general case where the bound chloride concentration depends on the concentrations of the other species, that is, $C_{bi} = C_{bi}(C_{fj})\ \forall j = 1,\ldots,n$, the matrixes $\boldsymbol{M}_{ij}$, $\boldsymbol{K}_{ii}$ and $\boldsymbol{K}_{ij}$ read:

$$\boldsymbol{M}_{ij} = \int_\Omega \left(1 + \frac{\partial C_{bi}}{\partial C_{fj}}\right)\left(\boldsymbol{N}^T\boldsymbol{N}\right) d\Omega \tag{37}$$

$$\boldsymbol{K}_{ii} = \int_\Omega D_i\left(1 + C_i^h\left[\gamma_i^{-1}\frac{\partial\gamma_i}{\partial C_i} - \frac{E_i}{\overline{\Phi}}\right]\right)\left((\nabla\boldsymbol{N})^T\,\nabla\boldsymbol{N}\right) d\Omega \tag{38}$$

$$\boldsymbol{K}_{ij} = \int_\Omega D_i C_i^h\left[\gamma_i^{-1}\frac{\partial\gamma_i}{\partial C_j} - \frac{E_j}{\overline{\Phi}}\right]\left((\nabla\boldsymbol{N})^T\,\nabla\boldsymbol{N}\right) d\Omega \tag{39}$$

where E_i and $\overline{\Phi}$ are defined as:

$$E_i = D_i\frac{z_i}{M_i}\left(1 + C_i^h\gamma_i^{-1}\frac{\partial\gamma_i}{\partial C_i}\right) + \sum_{j=1}^{n} D_j\frac{z_j C_j^h}{M_j\gamma_j}\frac{\partial\gamma_j}{\partial C_i} \tag{40}$$

$$\overline{\Phi} = \sum_{j=1}^{n} D_j\frac{z_j^2}{M_j}C_j^h \tag{41}$$

and $C_i^h = \boldsymbol{N}\cdot\boldsymbol{C}_i$.

6. Results and discussion

The three models are applied to the experimentally data obtained in section 3 and the results are discussed.

6.1. Apparent diffusion

The analytic solution of the apparent diffusion model (equation 34) is fitted to the experimental data obtained in section 3. This analysis provides the surface concentration and apparent diffusion coefficients which are listed in table 2. The corresponding chloride profiles are plotted in figure 1.

Table 2: Surface concentrations and apparent diffusion coefficients from the fitting analyses.

	Material SR		Material SF	
Days	C_{ts}	$D_a \times 10^{-12}$	C_{ts}	$D_a \times 10^{-12}$
182	10.7579	15.9201	10.5830	4.5850
364	10.0936	28.4170	11.3028	2.5625
546	10.2290	27.2258	11.0185	2.3356

It may be observed that the apparent diffusion coefficients listed in table 2 vary significantly and cannot be interpreted as intrinsic coefficients. This is mainly due to the non-linear chloride binding. The $R-squared$ values of each fit are shown in table 3.

Although the fits are very good, the model is not suitable for predicting the chloride penetration, as the value of the apparent diffusion coefficient is unknown a priori.

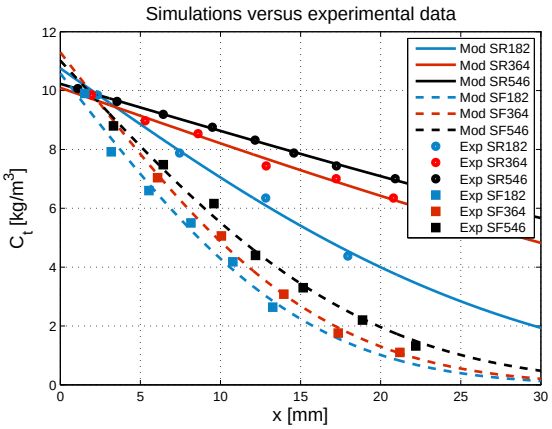

Figure 1: Experimental data versus the apparent diffusion model.

Table 3: $R-squared$ values of the fits.

Time (days)	Material SR	Material SF
182	0.9940	0.9830
364	0.9878	0.9961
546	0.9985	0.9924

6.2. *Effective diffusion*

In order to apply the effective diffusion model to the experimental data, the material parameters need to be well defined. The initial chloride content was calculated from the cement composition and dosage of the concretes. The binding isotherms were determined experimentally as described in section 3. The effective diffusion coefficients were determined as described in subsection 6.3. The experimentally obtained parameters are presented in table 4.

Table 4: Material parameters.

Material	SR	SF
C_{t0}	0.0380	0.0684
$D_e \times 10^{-11}$	2.84	1.02
ϕ (%)	14.5	12.5
C_{bm}	9.07	12.34
K_{eq}	2.13	0.72

The model accounts for the porosity changes due to the formation of Friedel's salt. As Friedel's salt forms, the porosity is reduced by the volume Friedel's salt occupies. The porosity can change in early times, due to the hydration of the materials. The overall porosity of material SR did not show important variations over time. However, according to the experimental study in (37), the overal porosity of material SF decreased more than 18% of its initial value in 18 months. This was accounted for by introducing a time dependent porosity. The latter varies linearly with time reducing the porosity by 18% of its initial value for the first 18 months, according to the experimental results obtained in (37).

Using the parameters listed in table 4, several simulations were performed by imposing a 3% *NaCl* solution on the boundary of the concrete samples for 182, 364, and 546 days. The results for both materials are plotted in figures 2-3. It may be observed that the constant diffusion coefficient D_e can be interpreted as an intrinsic coefficient, as the numerical solutions are in good agreement with the experimental data. Therefore, one can conclude that diffusion and chloride binding are the main transport mechanisms of chloride ions in saturated concrete. It is obvious that a precise knowledge of the binding capacity of the materials is essential. The numerical solutions for the total, free and bound chloride profiles for both materials at 546 days are plotted in figure 4.

The effective diffusion coefficient can be expressed as the product of the self-diffusion coefficient D_i^{μ} (constant for a given temperature) of species i and the dimensionless tortuosity-connectivity parameter τ (28). The latter takes values between 0 and 1. The smaller τ, the more tortuous and the less connected the pores of the medium. The parameter τ is given for both materials in table 5. Material SF appears to be much more tortuous and/or less connected than material SR.

Table 5: Tortuosity-connectivity parameters of the materials.

Material	SR	SF
τ	0.014	0.005

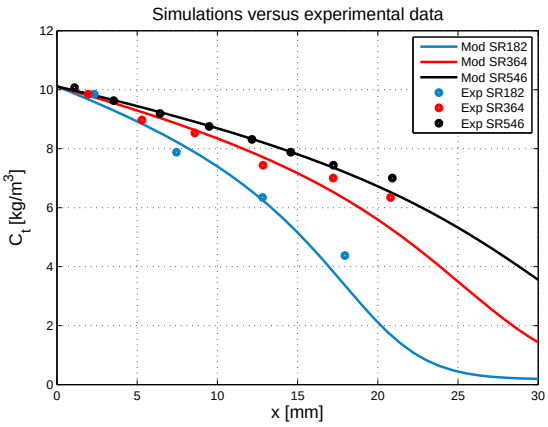

Figure 2: Experimental data versus the effective diffusion model for material SR.

It has been shown that the effective diffusion model presents good results. This model is suitable for predicting the chloride penetration in saturated concrete as it requires a constant diffusion coefficient as input. If the model described in subsection 6.1 were to be used with a constant diffusion coefficient at any time, it is obvious that the results would not be sufficient. To illustrate this, the chloride profiles calculated with the apparent diffusion model at 182, 364 and 546 days are plotted in figure 5. The apparent diffusion coefficient was chosen to be the one at 546 days for the material SR (see table 2). It may be observed that the chloride profile calculated by means of the apparent diffusion model at 182 days significantly overestimates the real

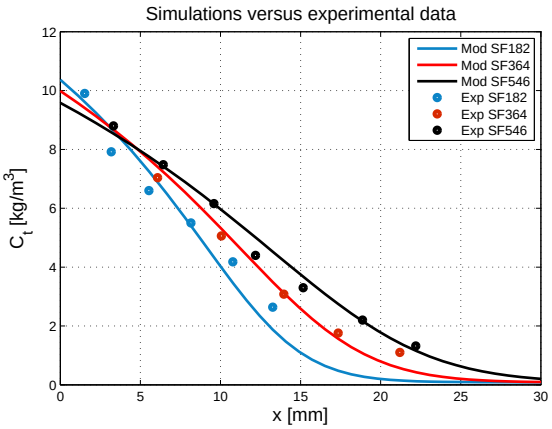

Figure 3: Experimental data versus the effective diffusion model for material SF.

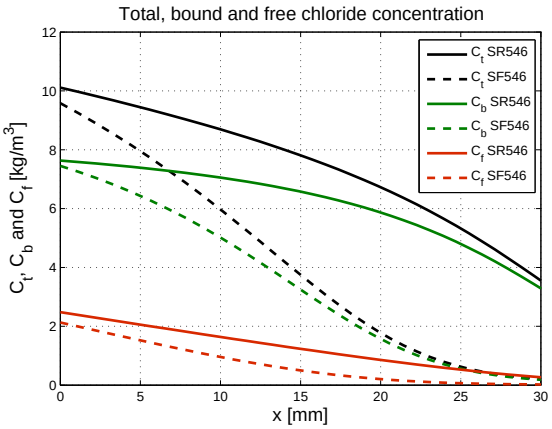

Figure 4: Total, bound and free chloride concentrations in kg/m^3 of concrete for both materials after 546 days of diffusion.

chloride concentration. It is probably due to 182 days is a very short period of time for natural chloride difussion in concrete.

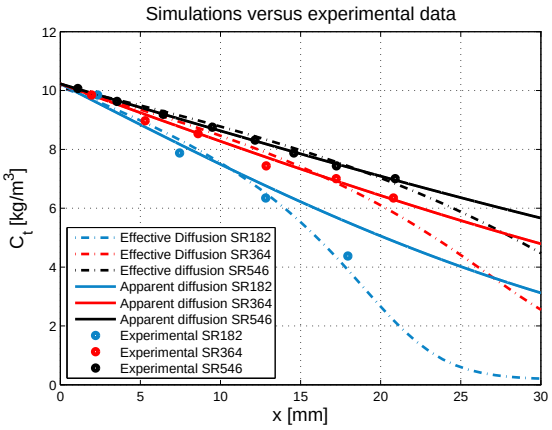

Figure 5: Comparison between the apparent and effective diffusion models.

In the next subsection, the numerical solutions are slightly enhanced by accounting for the ionic interactions between the species present in the pore solution.

6.3. Diffusion, activity and migration

In this subsection, the diffusion-activity-migration model is applied to the experimental data obtained in section 3. As for the effective diffusion model, a solution of 3% $NaCl$ is imposed on the Dirichlet boundary for 546 days. The same values for the porosity and the initial chloride concentration as in the previous subsection are adopted (see tables 4 and 5).

The ionic species considered in this model are Na^+, K^+, Ca^{2+}, Cl^- and OH^-. Sulfates are present at the first stage of the hydration process of concrete, but become negligible afterwards (49). In order to determine the initial concentration of each ionic compound, it is assumed that the oxides Na_2O and K_2O of the cements are entirely dissolved in the pore solution due to their limited content and high solubility. The initial chloride content is assumed to come from dissolved $NaCl$. The initial dissolved chloride concentration was obtained from the total initial chloride concentrations listed in table 4. Making use of the binding isotherms, the initial chloride concentration C_{Cl0} can be calculated by solving the following second order polynomial:

$$K_{eq}\phi^2 C_{Cl0}^2 + \phi\left(1 + K_{eq}\left[C_{bm} - C_{t0}\right]\right)C_{Cl0} - C_{t0} = 0 \qquad (42)$$

The corresponding initial concentration of Na^+ (coming from dissolved $NaCl$) is then:

$$C_{Na0} = \frac{M_{Na}}{M_{Cl}} C_{Cl0} \qquad (43)$$

where M_i is the molar mass species i.

The initial concentrations of the alkalis Na^+ and K^+ (coming from the Na_2O and K_2O compounds) were determined based on the research work (49). Since calcium oxide is abundantly present in cement, the initial concentration of the Ca^{2+} was determined by calculating the solubility of portlandite ($Ca(OH)_2$) in the $Na_2O - K_2O - NaCl - H_2O$ system. This is done by solving the equilibrium equation:

$$K_{sp} - a_{Ca}a_{OH}^2 = 0 \qquad (44)$$

where K_{sp} is the solubility product of portlandite and a_i is the activity of species i which depends on the concentrations of the ions present in the pore solution and is calculated with the Pitzer model. Finally, the initial OH^- concentration was calculated by imposing the electroneutrality condition. The initial concentration of each species is presented in table 6.

Table 6: Initial chemical composition of the pore solution in g/l of pore solution.

Material	$Na^{+(*)}$	K^+	Ca^{2+}	Cl^-	OH^-
SR	2.3075	9.7558	0.0345	0.0131	5.9744
SF	2.3353	9.7558	0.0342	0.0560	5.9742

$^{(*)}$ The Na^+ content comes from both the $NaCl$ and Na_2O molecules.

Chloride ions are assumed to bind to the cement matrix in the same way as in the previous subsection. However, assum-

ing that only chloride ions bind to the cement matrix would be inconsistent with the electroneutrality condition. Indeed, it would engender an excess of positive charge in the pore solution. Therefore, it is assumed in this work that part of the sodium ions coming from the $NaCl$ molecules is bound physically to the cement matrix, and the dissolution and precipitation of the OH^- ions guarantees the electroneutrality of the pore solution. Van Mien et al. (25) observed that the physically bound chloride concentration ranges from 60% to 80% of the total bound chloride content. Therefore, in this paper, it is assumed that 80% of both the sodium and chloride ions (coming from $NaCl$) are bound physically, and 20% of the chloride ions is bound chemically. The binding isotherms can then be expressed as:

$$C_{bCl} = C_{bm}\frac{K_{eq}C_{fCl}}{1 + K_{eq}C_{fCl}} \tag{45}$$

$$C_{bNa} = 0.8C_{bm}\frac{K_{eq}C_{fNa}}{1 + K_{eq}C_{fNa}} \tag{46}$$

$$C_{bOH} = \frac{M_{OH}}{M_{Na}}C_{bNa} - \frac{M_{OH}}{M_{Cl}}C_{bCl} \tag{47}$$

where the values of C_{bm} and K_{eq} are listed in table 4.

Having defined the boundary and initial conditions, equations 36 and 44 are solved simultaneously for the content of Ca^{2+}. The ouput of the model are the concentration profiles of the species, their chemical activity, the pH of the pore solution, and the electric field.

The effective diffusion coefficients (see table 4) were obtained to the nearest $1 \times 10^{-13} m^2/s$ by fitting the finite element solution to the experimental data of both materials after 546 of diffusion. The goodness of the fit analyses was characterized by the coefficient of determination (see table 7).

Table 7: $R - squared$ values of the fits.

Material	SR	SF
R^2	0.9913	0.9876

The numerical solutions and experimental data are plotted in figures 7-8. The total, free and bound chloride profiles for both materials at 546 days are plotted in figure 9. To illustrate the difference between this model and the effective diffusion model, the chloride profiles obtained by means of both models are plotted in figure 6. It may be observed that the results of the diffusion-activity-migration model are more accurate than those of the effective diffusion model. This is mainly due to the electric field. Indeed, the influence of the chemical activity is negligible as shown in the next subsection.

The activity coefficient of chlorides is plotted in figures 10-11 for both materials at several times. The coefficients vary between $\sim 0.77 - 0.89$. The difference between the curves of the activity coefficient of chlorides versus depth for the concrete SR and SF, is due to the chlorides move much faster in the first. So the differences become larger as the ages are higher,

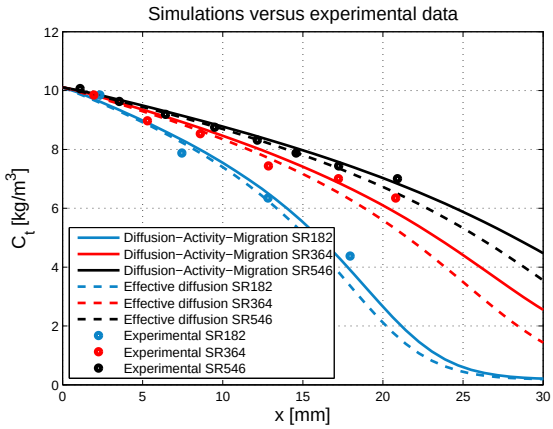

Figure 6: Comparison between the effective and the diffusion-activity-migration models.

since chloride penetration into the material SF for advanced age barely reaches 3 cm, while the in the case of material SR have come quite further. The same reason justifies the differences between the electric field for both materials which are shown in Figures 12 - 13 for several ages. In fact it can be seen in the figures as the maximum values of the activity coefficient and the minimum of the electric field occur almost the same depth x. The electric field is plotted in figures 12-13 for both materials at several times. The intensity of $\boldsymbol{E}$ decreases with time. Note that, since the electric field is negative everywhere, it repels the chloride ions. The maximum value of $-\boldsymbol{E}$ moves to greater depths with time. Denoting the depth at which the intensity of the electric field reaches its maximum at a given time as x_m ($E(x_m) = min_x \boldsymbol{E}$), the penetration velocity of chloride ions at depths $x < x_m$ is slown down, while the opposite is true for depths $x > x_m$.

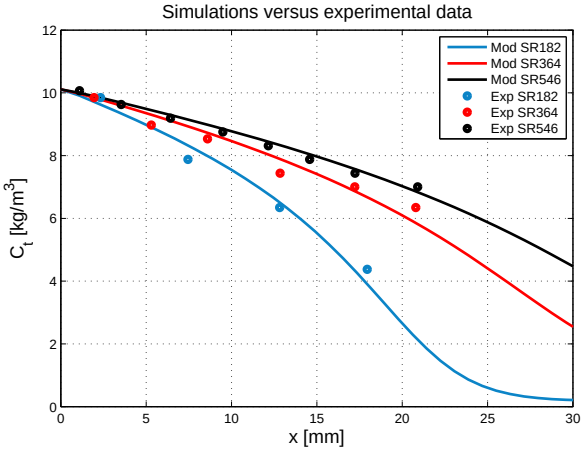

Figure 7: Experimental data versus the diffusion-activity-migration model for material SR.

6.4. *Influence of the chemical activity and the electric field*

In order to illustrate the influence of the chemical activity and migration on chloride penetration, three simulations are performed and compared. All the simulations are run with the

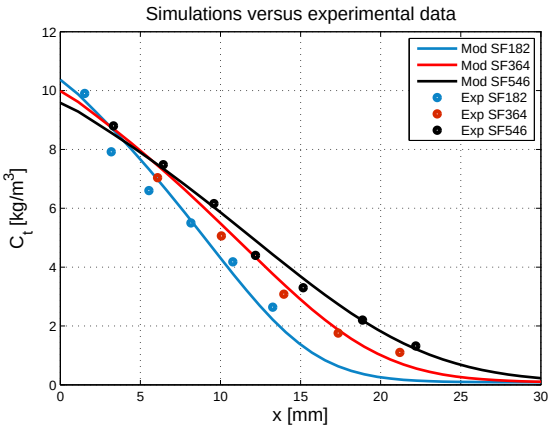

Figure 8: Experimental data versus the diffusion-activity-migration model for material SF.

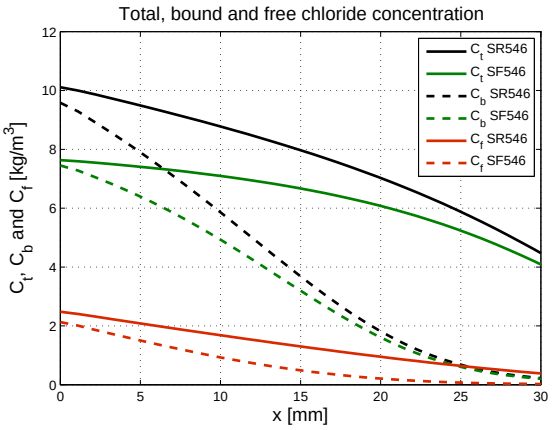

Figure 9: Total, bound and free chloride concentrations in kg/m^3 of concrete for both materials after 546 days of diffusion.

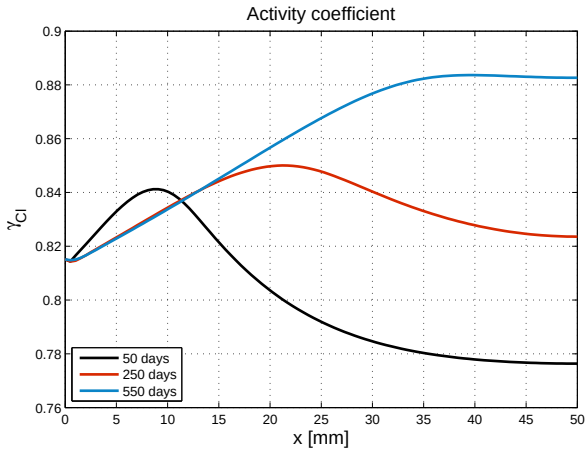

Figure 10: Activity coefficient γ_{Cl} for material SR at several times.

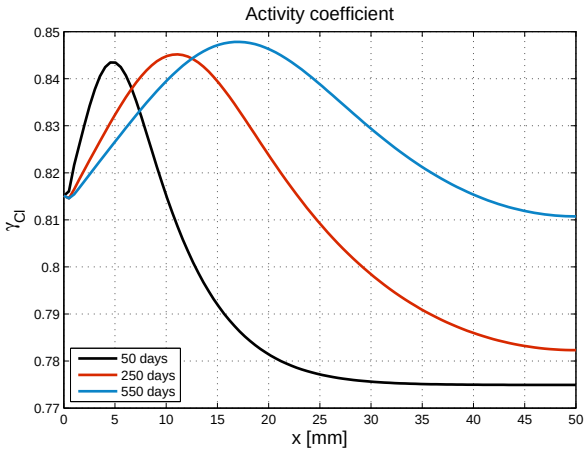

Figure 11: Activity coefficient γ_{Cl} for material SF at several times.

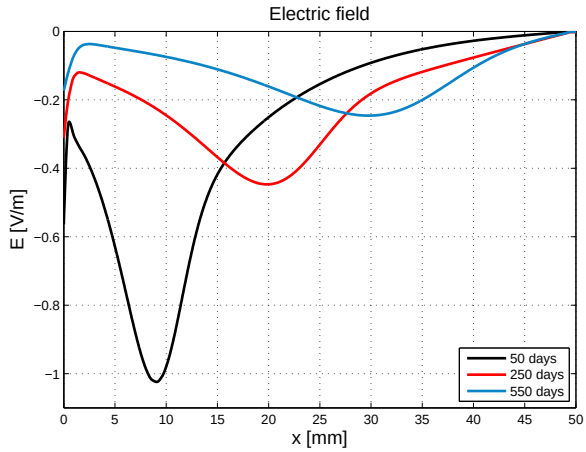

Figure 12: Electric field for material SR at several times.

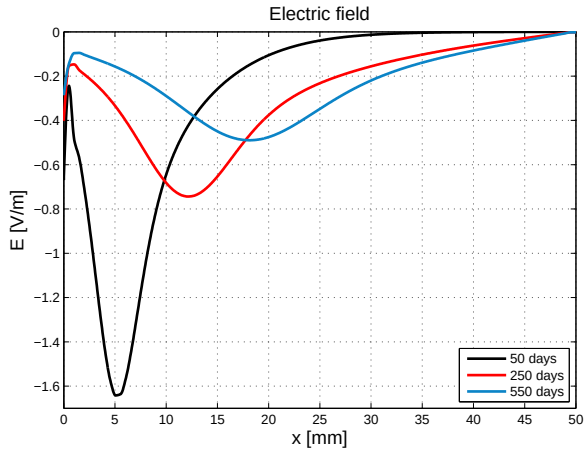

Figure 13: Electric field for material SF at several times.

same material (SR) and ion binding is ignored. A constant *NaCl* concentration of 3% is imposed on the boundary for 50 days. The first simulation accounts solely for diffusion, the second takes into account diffusion and migration, while the last one considers diffusion, chemical activity and migration. The chloride profiles are plotted in figure 14. It may be observed that migration affects visibly the chloride penetration, while the chemical activity can be ignored. The same can be said for the sodium ions. However, the effect of the electric field and chemical activity on the other ionic species is more significant. As an example, the hydroxide profiles are plotted in figure 15.

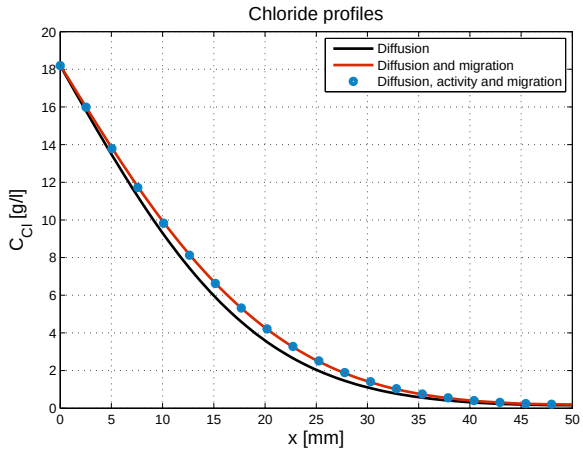

Figure 14: Chloride profiles: comparison between diffusion, chemical activity and migration.

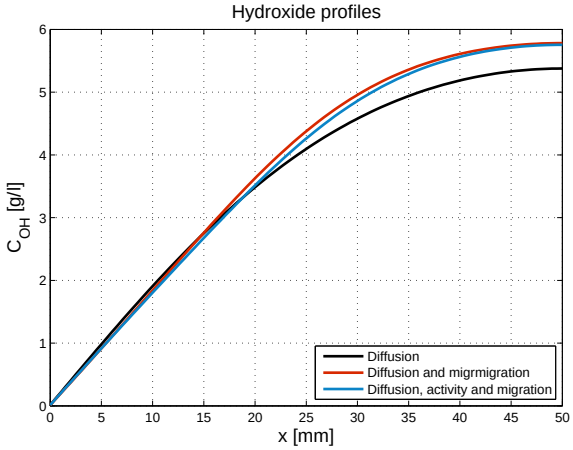

Figure 15: Hydroxide profiles: comparison between diffusion, chemical activity and migration.

7. Conclusions

This work proposes a multi-ionic transport model for saturated materials dedicated specifically to cementitious materials. The model accurately predicts the transport of chlorides inside reinforced concrete in order to study the processes involved in chloride induced corrosion, but that eventually may be used to predict the behaviour of concrete in several environments. In this study, several models for chloride transport in saturated concrete are revised and compared. The analyses carried out lead to the following conclusions:

1. The proposed model which couples the transport equations of ionic species in concrete with the Pitzer model allows to simulate the transport of the ionic species present in the pore solution taking into account diffusion, migration and chemical activity. The output of the model are the concentration profiles of all the ionic species present in the pore solution (total, free and bound), the pH of the pore solution, the electric field, the chemical activity and the activity coefficient.
2. The proposed model that couples the Pitzer's model, the chemical activity and the migration leads to a more accurate results, but requires additional effort to obtain the involved parameters. At time of writting this paper, the authors do not know any other proposal of the coupled model. The paper also provides the study of the accuracy of such a model.
3. Modelling chloride penetration by means of the apparent diffusion model with a constant apparent diffusion coefficient provides results that may be improved. The apparent diffusion coefficient can be calculated by fitting the analytic solution of the apparent diffusion model to experimentally obtained chloride profiles. The so obtained value of D_a is difficult to interpret, as it does not solely depend on the microstructure of the material, but also on its binding capacity.
4. The effective diffusion model with a constant effective diffusion coefficient leads to better results. It is essential to determine the bound chloride content with high accuracy.
5. The diffusion-activity- migration model enhances slightly the results obtained with the effective diffusion model. The concentration and chemical activity of every species present in the pore solution as well as the electric field can be determined at any point and at any time. These may be used to study the mechanisms involved in several processes of deterioration. However, the fully coupled model is more complex to implement and needs more computational effort.
6. The electric field significantly affects the penetration of ionic species.
7. The effect of chemical activity on chloride and sodium transport appeared to be negligible, whereas the other species seemed to be more affected. If the chloride ions are the ionic species of interest, the chemical activity can be ignored and coupling the transport equations to the Pitzer model can be omitted.
8. The proposed model and the result obtained provide the way of comparison of experimental results of chloride transport in concrete obtained with different testing procedures and standards.

8. Acknowledgements

The authors gratefully acknowledge the financial support provided for this research by the Spanish Ministerio de Economía y Competitividad under grant BIA2016-78742-C2-2-R.

References

[1] C. Page, M. Page (2007). doi:https://doi.org/10.1533/9781845693398.1.
[2] S. Mahmoud Abdelkader, E. Reyes Pozo, A. Moragues Terrades, Evolution of microstructure and mechanical behavior of concretes utilized in marine environments, Materials & Design 31 (7) (2010) 3412 – 3418.
[3] E. Samson, J. Marchand, Modeling the transport of ions in unsaturated cement-based materials, Computers & Structures 85 (23) (2007) 1740 – 1756. doi:https://doi.org/10.1016/j.compstruc.2007.04.008.

[4] J. Bernal, M. Fenaux, A. Moragues, E. Reyes, J. Gálvez, Study of chloride penetration in concretes exposed to high-mountain weather conditions with presence of deicing salts, Construction and Building Materials 127 (Supplement C) (2016) 971 – 983. doi:https://doi.org/10.1016/j.conbuildmat.2016.09.148.

[5] S. Guzmán, J. C. Gálvez, J. M. Sancho, Modelling of chloride ingress into concrete through a single-ion approach. application to an idealized surface crack pattern, International Journal for Numerical and Analytical Methods in Geomechanics 38 (16) (2014) 1683–1706, nAG-13-0140.R1. doi:10.1002/nag.2273.

[6] T. J. Kirkpatrick, R. E. Weyers, C. M. Anderson-Cook, M. M. Sprinkel, Probabilistic model for the chloride-induced corrosion service life of bridge decks, Cement and Concrete Research 32 (12) (2002) 1943 – 1960. doi:https://doi.org/10.1016/S0008-8846(02)00905-5.

[7] Y. Wang, L. yuan Li, C. Page, Modelling of chloride ingress into concrete from a saline environment, Building and Environment 40 (12) (2005) 1573 – 1582. doi:https://doi.org/10.1016/j.buildenv.2005.02.001.

[8] A. Guimarães, M. Climent, G. de Vera, F. Vicente, F. Rodrigues, C. Andrade, Determination of chloride diffusivity through partially saturated portland cement concrete by a simplified procedure, Construction and Building Materials 25 (2) (2011) 785 – 790, composite Materials and Adhesive Bonding Technology. doi:https://doi.org/10.1016/j.conbuildmat.2010.07.005.

[9] O. Vennesland, M. Climent, C. Andrade, Recommendation of rilem tc 178-tmc: Testing and modelling chloride penetration in concrete (2013-03).

[10] A. Saetta, R. Scotta, R. Vitaliani, Analysis of Chloride Diffusion into Partially Saturated Concrete, Materials Journal 90 (5) (1993) 441 – 451.

[11] A. Suryavanshi, J. Scantlebury, S. Lyon, Mechanism of Friedel's salt formation in cements rich in tri-calcium aluminate, Cement and Concrete Research 26 (5) (1996) 717 – 727.

[12] U. Birnin-Yauri, F. Glasser, Friedel's salt, $Ca_2Al(OH)_6(Cl,OH)\cdot 2H_2O$: its solid solutions and their role in chloride binding, Cement and Concrete Research 28 (12) (1998) 1713 – 1723.

[13] O. Jensen, M. Korzen, H. Jakobsen, J. Skibsted, Influence of cement constitution and temperature on chloride binding in cement paste, Advances in cement research 12 (2) (2000) 57–64.

[14] Q. Yuan, C. Shi, G. D. Schutter, K. Audenaert, D. Deng, Chloride binding of cement-based materials subjected to external chloride environment – A review, Construction and Building Materials 23 (1) (2009) 1–13.

[15] M. Masi, D. Colella, G. Radaelli, L. Bertolini, Simulation of chloride penetration in cement-based materials, Cement and Concrete Research 27 (10) (1997) 1591 – 1601, materials Research Society Symposium on Structure-Property Relationships in Hardened Cement Paste and Composites. doi:https://doi.org/10.1016/S0008-8846(97)00200-7.

[16] E. Samson, J. Marchand, Numerical Solution of the Extended Nernst-Planck Model, Journal of Colloid and Interface Science 215 (1) (1999) 1 – 8.

[17] Y. Yang, M. Wang, Pore-scale modeling of chloride ion diffusion in cement microstructures, Cement and Concrete Composites 85 (Supplement C) (2018) 92 – 104. doi:https://doi.org/10.1016/j.cemconcomp.2017.09.014.

[18] C. Page, N. Short, A. E. Tarras, Diffusion of chloride ions in hardened cement pastes, Cement and Concrete Research 11 (3) (1981) 395 – 406.

[19] S. Goto, D. Roy, Diffusion of ions through hardened cement pastes, Cement and Concrete Research 11 (5-6) (1981) 751 – 757.

[20] L. Tang, Chloride transport in concrete - measurement and prediction, Ph.D. thesis, Chalmers University of Technology, Gothenburg, Sweden (1996).

[21] K. Tuutti, The corrosion of steel in concrete, Ph.D. thesis, Swedish Cement and Concrete Research Institute (CBI), Stockholm, Sweden (1982).

[22] L. Tang, L.-O. Nilsson, Chloride binding capacity and binding isotherms of OPC pastes and mortars, Cement and Concrete Research 23 (2) (1993) 247 – 253.

[23] H. Zibara, R. Hooton, M. Thomas, K. Stanish, Influence of the C/S and C/A ratios of hydration products on the chloride ion binding capacity of lime-SF and lime-MK mixtures, Cement and Concrete Research 38 (3) (2008) 422 – 426.

[24] T. Nguyen, V. Baroghel-Bouny, P. Dangla, P. Bein, Numerical modelling of chloride ingress into saturated concrete, in: Second International Symposium on Advances in Concrete through Science and Engineering, RILEM Proceedings, Vol. 51, RILEM Publications, Quebec City, Canada, 2006.

[25] T. Van Mien, B. Stitmannaithum, T. Nawa, K. Kurumisawa, N. Van Chanh, Contributions of C-S-H and AFm hydrates to chloride binding isotherms of various cements, in: The 3^{rd} ACF International Conference - ACF/VCA, 2008.

[26] P. Iqbal, T. Ishida, Modeling of chloride transport in concrete coupled with moisture migration in marine environment based on thermodynamic approach, in: The International Symposium on Social Management Systems, Yichan, China, 2007.

[27] O. Coussy, F. Ulm, Elements of durability mechanics of concrete structures, in: F. Ulm, Z. Bažant, F. Wittmann (Eds.), Creep, Shrinkage and Durability Mechanics of Concrete and other Quasi-Brittle Materials, Elsevier, Oxford, United Kingdom, 2001, pp. 393–409.

[28] E. Samson, J. Marchand, J. Beaudoin, Describing ion diffusion mechanisms in cement-based materials using the homogenization technique, Cement and Concrete Research 29 (8) (1999) 1341 – 1345.

[29] L. Tang, Concentration dependence of diffusion and migration of chloride ions: Part 2. experimental evaluations, Cement and Concrete Research 29 (9) (1999) 1469 – 1474. doi:http://dx.doi.org/10.1016/S0008-8846(99)00120-9.

[30] J. Marchand, B. Gérard, A. Delagrave, Ion transport mechanisms in cement-based materials, in: Materials Science of Concrete, Vol. 5, American Ceramic Society, 1998, pp. 307–400.

[31] K. S. Pitzer, Theoretical considerations of solubility with emphasis on mixed aqueous electrolytes, Pure & Applied Chemistry 58 (12) (1986) 1599–1610.

[32] E. Samson, G. Lemaire, J. Marchand, J. Beaudoin, Modeling chemical activity effects in strong ionic solutions, Computational Materials Science 15 (3) (1999) 285 – 294.

[33] O. Truc, J.-P. Ollivier, L.-O. Nilsson, Numerical simulation of multi-species transport through saturated concrete during a migration test - msdiff code, Cement and Concrete Research 30 (10) (2000) 1581 – 1592. doi:http://dx.doi.org/10.1016/S0008-8846(00)00305-7.

[34] M. Fenaux, Modelling of chloride transport in non-saturated concrete. From Microscale to Macroscale, Ph.D. thesis, Escuela Téecnica Superior de Ingenieros de Caminos, Canales y Puertos, Madrid, Spain (May 2013).

[35] Instrucción para la recepción de cementos (RC-16), AENOR, 2008.

[36] Ministry of the Presidency, Madrid, Spain, EHE - Code on Structural Concrete (August 2008).

[37] S. Mahmoud Abdelkader, Influencia de la composición de distintos hormigones en los mecanismos de transporte de iones agresivos procedentes de medios marinos, Ph.D. thesis, Escuela Técnica Superior de Ingenieros de Caminos, Canales y Puertos, Madrid, Spain (Juin 2010).

[38] ASTM C1543-02 Standard Test Method for Determining the Penetration of Chloride Ion into Concrete by Ponding, ASTM International, West Conshohocken, PA, United States, 2002.

[39] UNE 112010:1994, Corrosión de armaduras. Determinación de cloruros en hormigones endurecidos y puestos en servicio, AENOR, 1994.

[40] M. Castellote, C. Andrade, TC 178-TMC: Testing and modelling chloride penetration in concrete. Round-Robin test on chloride analysis in conrete – Part II: Analysis of water soluble chloride content, Materials and Structures 34 (244) (2001) 589–598.

[41] Effect of supplementary cementing materials on concrete resistance against carbonation and chloride ingress, Cement and Concrete Research 30 (2) (2000) 291 – 299.

[42] A. Moragues, A. Macias, C. Andrade, Equilibria of the chemical composition of the concrete pore solution. Part I: Comparative study of synthetic and extracted solutions, Cement and Concrete Research 17 (2) (1987) 173 – 182.

[43] A. Moragues, A. Macias, C. Andrade, J. Losada, Equilibria of the chemical composition of the pore concrete solution Part II: Calculation of the equilibria constants of the synthetic solutions, Cement and Concrete Research 18 (3) (1988) 342 – 350.

[44] P. Debye, E. Hückel, Zur Theorie der Elektrolyte, Physikalische Zeitschrift 24 (9) (1923) 185–206.

[45] P. Marliacy, N. Hubert, L. Schuffenecker, R. Solimando, Use of Pitzer's model to calculate thermodynamic properties of aqueous electrolyte solutions of Na2SO4+NaCl between 273.15 and 373.15K, Fluid Phase Equilibria 148 (1998) 95–106.

[46] A. Dinane, Thermodynamic properties of NaCl-NH4Cl-LiCl-H2O at

T=298.15K, Fluid Phase Equilibria 273 (1-2) (2008) 59–67.

[47] J. H. G. van der Stegen, H. Weerdenburg, A. J. van der Veen, J. A. Hogendoorn, G. F. Versteeg, Application of the Pitzer model for the estimation of activity coefficients of electrolytes in ion selective membranes, Fluid Phase Equilibria 157 (2) (1999) 181–196.

[48] M. Boufadel, M. Suidan, A. Venosa, A numerical model for density-and-viscosity-dependent flows in two-dimensional variably saturated porous media, Journal of Contaminant Hydrology 37 (1999) 1–20.

[49] M. T. Gaztañaga Colom, Influencia de la carbonatación en la microestructura de diferentes pastas de cemento hidratadas, Ph.D. thesis, Universidad Complutense de Madrid, Madrid,Spain (1996).